



## Research Article

# Cross linked Core-shell Silica Nanoparticles Mechanical, Structural & Viscoelastic Behavior

K. M. Faridul Hasan<sup>1,\*</sup>, Mst. Zakia Sultana<sup>2</sup>, Ashaduzzaman<sup>2</sup>,

Md. Shipan Mia<sup>2</sup>, Md. Mostafizur Rahman<sup>2</sup>, Muhammad Abu Taher<sup>2</sup>

<sup>1</sup>School of Textile Science & Engineering, Wuhan Textile University, Wuhan, China

<sup>2</sup>School of Textile Chemistry & Chemical Engineering, Wuhan Textile University, Wuhan, China

### Abstract

Shell cross-linked core-shell nanoparticles (SCCSNs) were prepared via miniemulsion polymerization of styrene in the presence of silane modified inorganic silica. The polystyrene (PS) shell of 69.8% in weight fraction was cross-linked using divinylbenzene. SCCSNs were spherical with a diameter distribution from 37 to 96 nm determined by dynamic light scattering. Dynamic rheology of SCCSNs suspended in PS/toluene solution was compared with that of suspensions of naked silica. The critical strain for onset of rheological nonlinearity was independent of SCCSN concentration above a concentration threshold, which differs from the silica suspensions. Linear dynamic rheological investigation revealed that SCCSN suspensions with a PS volume fraction of 25% were fluid-like at low particle concentrations while suspensions containing 4.5 vol% SCCSNs formed a gel-like structure. On the contrary, the silica suspensions with 20.0 vol% PS underwent a fluid-to-solid-like transition with increasing silica concentration. Reasons for the different rheological behaviors of the naked silica and SCCSN suspensions are discussed.

**Keywords:** core-shell nanoparticles; polymerization; polystyrene; suspension; Crosslink

**Academic Editor:** Taihong Shi, PhD, Department of Environment Science, Sun Yat-sen University, China

**Received:** October 7, 2016; **Accepted:** November 24, 2016; **Published:** December 20, 2016

**Copyright:** 2016 Hasan KMF *et al.* This is an open-access article distributed under the terms of the Creative Commons Attribution License, which permits unrestricted use, distribution, and reproduction in any medium, provided the original author and source are credited.

**\*Correspondence to:** K. M. Faridul Hasan, School of Textile Science & Engineering, Wuhan Textile University, Wuhan, China

**E-mail:** farid\_textile@yahoo.com

## 1. Introduction

Polymer nanocomposites have attracted considerable industrial and academic interest due to their remarkable mechanical, thermal, electrical and gas barrier properties and their extensive application prospects in water-resistant, durable, anti-pollution coatings and in multi-function membrane materials [1]. Coatings filled with nanoparticles can obviously improve weather and abrasive resistances, and mechanical, antibacterial and photocatalytic activity properties. Stability of nanoparticles suspended in polymer solutions has a great impact on the preparation of coatings and multi-function membrane materials [2, 3]. However, due to their small size, large specific surface area and high surface energy, nanoparticles are easy to agglomerate, which will seriously affect the rheological behavior of nanoparticle suspensions and lead to poorer functional properties of the final materials. It is thus of importance to improve the dispersion stability of nanoparticle suspensions [4, 5].

Core-shell nanoparticles prepared via suspension, emulsion, dispersion and miniemulsion polymerizations are superior in modifying surface wetting and improving dispersibility in comparison with naked nanoparticles.<sup>25</sup> Miniemulsion polymerization is a reliable technique for yielding high encapsulation efficiency and the size of core-shell nanoparticles can be easily adjusted by adjusting surfactant concentration and shear intensity during polymerization[6] [7]. Titanium dioxide (TiO<sub>2</sub>), calcium carbonate (CaCO<sub>3</sub>) and precipitated silica (SiO<sub>2</sub>) nanoparticles encapsulated with polystyrene (PS) with a high encapsulation efficiency have been prepared via miniemulsion polymerization [8].

For nanoparticle suspensions, particle and particle-polymer interactions coexist, which influence dispersion stability and rheological behavior. Charge repulsion, surface polymer grafting and polyelectrolytes have been used to improve the dispersion stability of inorganic particle suspensions. However, nanoparticles in suspension can undergo a microstructural change attributed to a network-forming process via surface interaction [6, 9, 10]. Nano-SiO<sub>2</sub> has been widely used in adhesives, inks and coatings for its reinforcement and thickening properties so that a variety of core-shell SiO<sub>2</sub> nanoparticles have been reported. However, few investigations have been carried out to study rheological behaviors of core-shell SiO<sub>2</sub> nanoparticle suspensions. Recently, nanocomposite approaches have shown potential in overcoming the drawbacks of a polymeric hydrogel network [11]. Polymer nanocomposites possess superior properties compared to macro and micro-composites. Nanocomposites offer several novel property combinations such as high toughness, elastomeric properties, gas barrier, and control release due to the molecular interaction of fillers with polymers at the Nano scale[12].

In this article we prepared core-shell SiO<sub>2</sub> nanoparticles with a cross-linked PS shell via miniemulsion polymerization and investigated the dynamic rheology of the shell cross-linked core-shell nanoparticles (SCCSNs) suspended in PS/toluene solution[13, 14]. The cross-linked PS shell not only stabilizes the Nano silica core and prevents particle – particle interaction but also avoids macromolecules in the PS shell entangling with the PS present as dispersion phase with toluene [15]. Through comparing the suspension rheology of SCCSN and naked silica suspensions, we aimed to explore the influence of particle – polymer interfacial interaction on rheology behaviors of nanoparticle suspensions. Recently, silica-based nanoparticles have been extensively investigated for various biomedical and biotechnological applications such as analytical tools, imaging, and controlled drug release and delivery. This is mainly due to their unique optical properties, low density, high specific surface area, low toxicity and high adsorption capacity [16].

## 2. Experimental

### 2.1. Materials

Silica with an average primary particle size of 30 nm was purchased from Sinopharm Chemical Reagent company limited (China). Chemical pure grade styrene (St) was purified by distillation under reduced pressure before use. Coupling agent  $\gamma$ -methacryloxypropyl trimethoxysilane ( $\gamma$ -MPS) was purchased from Sinopharm Chemical Reagent company limited (China). PS (weight-average molecular weight of  $1.5 \times 10^5$  g mol<sup>-1</sup>) was purchased from Dow Chemical Co., USA. Sodium hydrogen carbonate (NaHCO<sub>3</sub>), sodium dodecylsulfate (SDS), divinylbenzene (DVB), absolute ethanol and potassium persulfate (KPS) of reagent grade were purchased from Tianjin Chemical Reagent Co., China and were used without further purification. Polyethylene glycol mono-p-nonyl phenyl ether (OP-10) from Sinopharm Chemical Reagent Company limited (China), and hexadecane (HD) co-stabilizer from Chengdu Kelong Chemical Reagent Co., China, were used as received. Other reagents were of chemical pure grade.

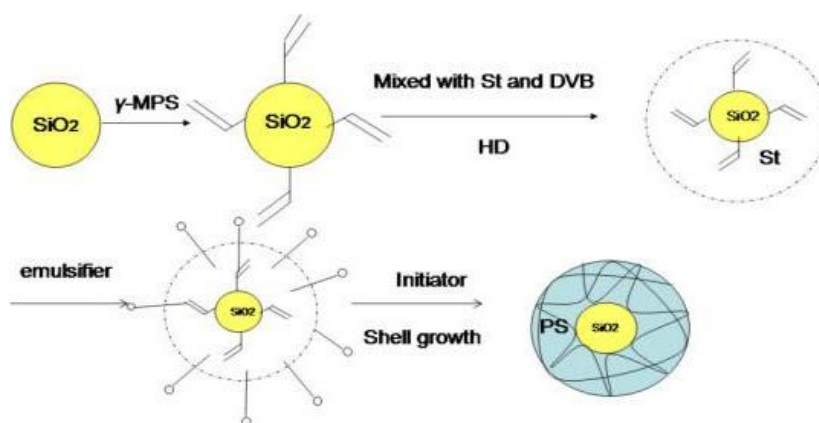


**Figure 1** Synthesis of Silica Nanoparticle

### 2.2. Methods

#### 2.2.1. Preparation of $\gamma$ -MPS-modified silica particles

Dried silica particles were treated using  $\gamma$ -MPS in toluene for 8 h at 110°C under stirring. The amount of  $\gamma$ -MPS was 5 wt% based on the amount of silica. After reaction, the silica suspension as shown in Figure 1 was centrifuged at 10,000 rpm for 40 min. The precipitates were carefully washed three times with ethanol and a further three times with deionized water in order to remove excess  $\gamma$ -MPS. The washed particles were dried overnight in a vacuum oven at 60°C.

#### 2.2.2. Preparation of SCCSNs

The synthesis process is shown in

Figure 1 In a typical experiment, 5 g of  $\gamma$ -MPS-modified silica powder was first dispersed in a mixture of 50 g of St, 2.5 g of HD and 2.5 g of DVB with the aid of ultrasound. The dispersion was introduced into a solution of 2.5 g of SDS, 0.5 g of OP-10 and 0.025 g of NaHCO<sub>3</sub> in 250 mL of water. After the mixture was stirred for 1 h, a miniemulsion was prepared by ultrasonication of the mixture for 15 min at 70% amplitude using an ultrasonicator.

The resultant miniemulsion was transferred into a 500 mL four-necked flask with a mechanical stirrer, a nitrogen inlet and a reflux condenser. After purging with nitrogen for 30 min, the polymerization reaction was initiated using 0.5 g of KPS at 60°C. After reaction at 80°C for 2.5 h, the mixture was poured into a breaker and 10 mL of 20% aqueous CaCl<sub>2</sub> solution was added. The product collected through suction filtration was washed with deionized water, tetrahydrofuran and ethanol in turn three times, and was dried at 60°C in vacuum for 12 h. The washing process removed SDS and other reagents used in the miniemulsion polymerization. The product was further extracted with boiling toluene at 110°C for 48 h in a Soxhlet apparatus to remove any ungrafted polymer, and was finally dried to constant weight in vacuum.

### 2.2.3. Preparation of nanoparticle suspensions

PS/toluene solutions at three volume concentrations,  $\phi_{PS}$ =8.5, 17.2 and 20.0 vol%, were prepared. A concentration  $\phi_{PS}$ =17.2 vol% was close to the critical entanglement concentration. Silica and SCCSNs were dispersed in the PS/toluene solutions under ultrasonication at room temperature. Concentrations of PS in toluene,  $\phi_{PS}$ , and concentrations of silica and SCCSNs in suspensions,  $\phi_{SiO_2}$  and  $\phi_{SCCSN}$ , were expressed in volume fraction taking densities of toluene, PS, silica as indicated in Figure 1 and SCCSNs as 0.865, 1.040, 1.800 and 1.226 g cm<sup>-3</sup>, respectively, at room temperature.

### 2.2.3. Characterization

FTIR Spectra of the colored polyester fabric is taken through Vertex 70 (Bruker) FTIR machines. TGA from 30 to 800°C was performed with a thermogravimetric analyzer (Pyris 1, PerkinElmer, USA) at a heating rate of 10°C min<sup>-1</sup> in nitrogen atmosphere. Diameters of SCCSN latexes were determined using dynamic light scattering at 25°C with a particle size analyzer (BI-90 plus, Brookhaven Instruments, USA). Scanning electron microscopy images were taken by using JSM-6510LV SEM machine.

The observation was performed after scattering the particles on a carbon conducting resin and spraying a thin gold layer. Transmission electron microscopy (TEM; JEM 1200EX, Electron, Japan) was used to observe the particle morphology. The latexes were diluted with deionized water and ultrasonicated for 5 min. One drop of suspension was diluted into water and was placed on a 400-mesh carbon-coated copper grid. TEM observation was performed after drying the grid. Dynamic frequency ( $\omega$ ) sweeps were performed from 0.01 to 100 rad s<sup>-1</sup> under 0.3% strain in the linearity region predetermined by performing strain sweeps from 0.01 to 100% using a rheometer (AR G2, TA Instruments, USA) at 25 °C in parallel-plate geometry. The uncertainty of critical strain  $\gamma_c$  for the onset of rheological nonlinearity was about  $\pm 15\%$ .

## 3. Results and Discussion

Quantitative analyses of the physically adsorbed and chemically cross-linked PS coverage on SCCSN surface were performed using TGA measurements, as shown in Fig. 2. The un extracted and extracted SCCSNs exhibit weight losses of 67.1 and 57.5 wt%, respectively, at temperatures from 350 to 600°C, revealing that a nanocomposite particle before toluene extraction contains about 5.9 wt% physically adsorbed PS chains. Residual weights of the SCCSNs before and after extraction are 37.9 wt% and 41.5 wt% at 800°C. Based on the TGA residues at 800°C, the weight content of crosslinked PS shell of the SCCSNs is estimated at about 59.6%.

SEM micrographs and size distributions of uncoated silica and SCCSNs are shown in Figure 2. The silica particles of about 30 nm tend to aggregate into large agglomerates due to interaction of silanol groups on particle surfaces. It is hard to clearly identify any agglomerate from SEM micrographs while a wide size distribution of 460 – 850 nm determined using dynamic light scattering can be easily ascribed to the silica agglomerates in extremely diluted medium.

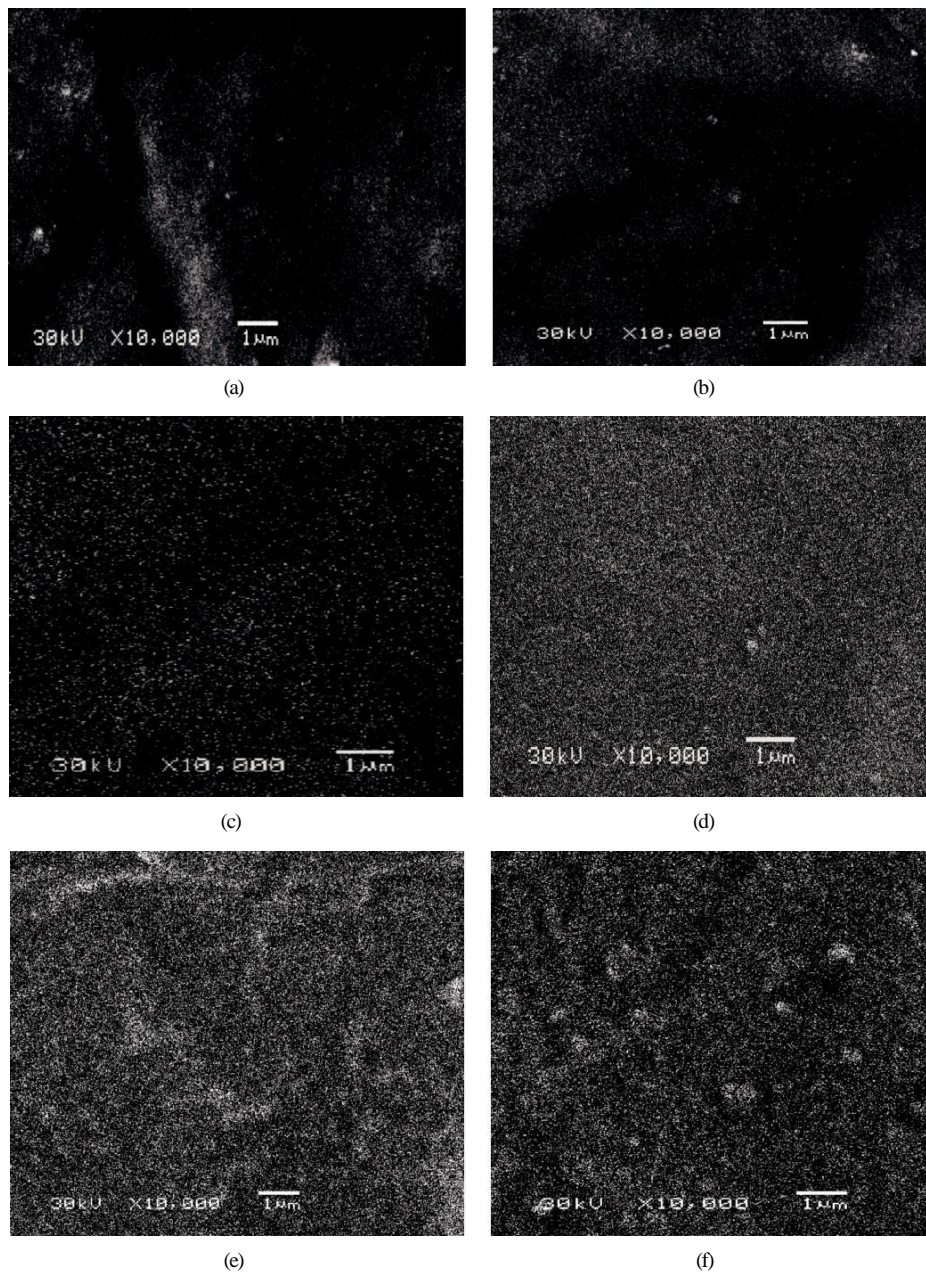


**Figure 2** SEM images showing the homogenous dispersion of the nano-SiO<sub>2</sub> ( $\times 10,000$ ). (a) 0.5% nano-SiO<sub>2</sub> (GII); (b) 1% nano-SiO<sub>2</sub> (GIII); (c) 1.5% nano-SiO<sub>2</sub> (GIV); (d) 2% nano-SiO<sub>2</sub> (GV); (e) 2.5% nano-SiO<sub>2</sub> (GVI); (f) 3% nano-SiO<sub>2</sub> (GVII).

SCCSNs are spherically shaped with a diameter of 32-98 nm and a most probable diameter of 66 nm, meaning that approximately 1-3 and most probably 2 beads cooperate in one SCCSN despite the unimodal dynamic light scattering curve.

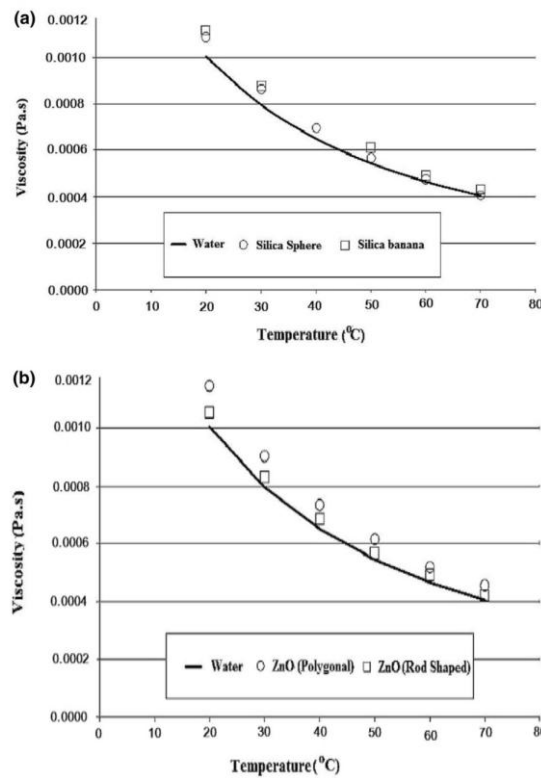


**Figure 3** (a) Viscosity of silica–water nanofluid; (b) viscosity of ZnO–water nanofluid

Suspensions exhibit nonlinear behavior and the nonlinearity becomes marked with increasing  $\phi_{SiO_2}$ , which is associated with release of trapped entanglement of PS macromolecules adsorbed on silica particles and breakdown of particle networks, because the PS macromolecules do not undergo disentanglement within the range of  $\gamma$  from 0.1 to 100%. The SCCSN suspensions with  $\phi_{PS} = 20.0$  vol% also exhibit nonlinear rheology (Figure 3) at  $\phi_{SCCSN} > 0.7$  vol% ascribed to desorption of physically adsorbed PS macromolecules from the crosslinked PS shell of SCCSNs. Figure 3 shows critical strain  $\gamma_c$  for the onset of nonlinear rheological behavior and  $G$  in the linearity region,  $G_0$ , as a function of  $\phi_{SiO_2}$  for silica suspensions or  $\phi_{SCCSN}$  for SCCSN suspensions. The silica concentration threshold is not detected in the suspensions of  $\phi_{PS} = 8.50$  and 20.0 vol% while it is located in the  $\phi_{SiO_2}$  range from 0.1 to 0.5 vol% for the silica suspension with  $\phi_{PS} = 17.2$  vol%.

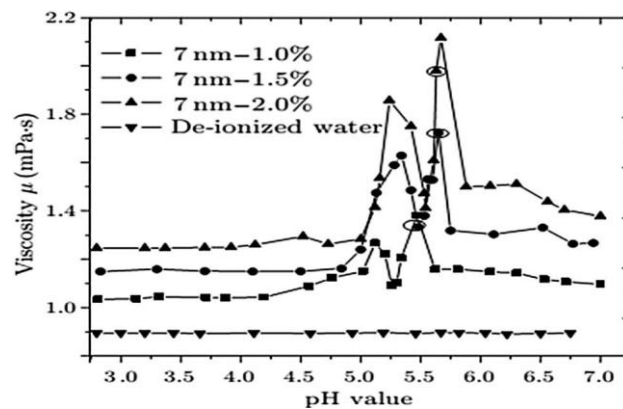


**Figure 4** Viscosity of Nano fluids (particle diameter = 7 nm) and de-ionized water vs.  $p^H$  value

Incorporation of silica ( $\text{SiO}_2$ ) filler into a silicone polymer is called compounding [27]. This is accomplished prior to cross-linking. The addition of silica filler is a vital factor in the physical and mechanical properties of silicone elastomers (

Figure 4), because the unfilled cross-linked polydimethyl siloxane (PDMS) has very low mechanical properties, since a very high cross-link density produces an inelastic brittle material. That made using silica fillers essential for enhancing the mechanical properties. The addition of surface treated silica fillers can augment the tensile strength of the cross-linked polymer by up to 40 times. The reason behind the increased strength is the strong physical and chemical bonds between the vulcanized polymer and the silica filler. Thus, polymer/filler interactions are maximized [17]. The hydrophobic surface treatment of the filler is also essential to prevent water absorption into the cured PDMS elastomer, since finished facial prostheses is subjected to sebum, sebaceous, and perspirations from the underlying living human skin which may lead to deterioration of the prosthesis [30].

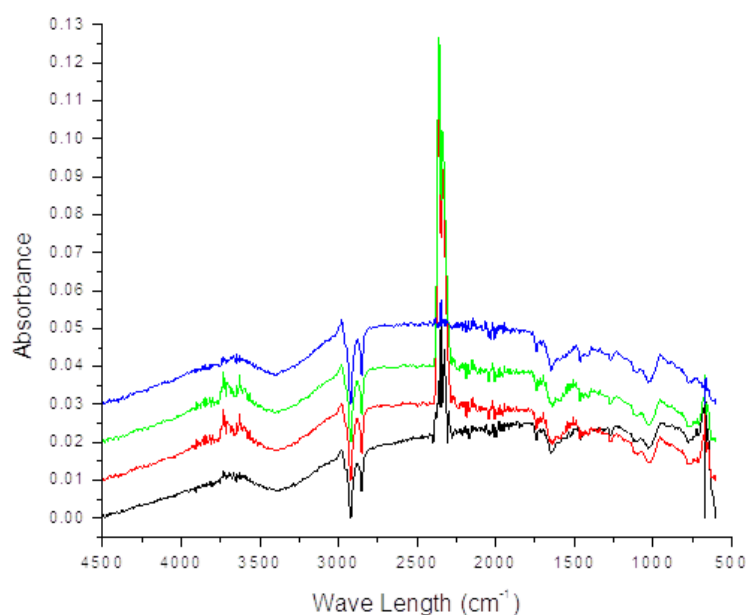


**Figure 5** FTIR Analysis of Silica Nanoparticles

FTIR and TGA were used to verify the encapsulation efficiency of SCCSNs. Figure 5 shows FTIR spectra of silica and SCCSNs. In comparison with the spectrum of silica, that of SCCSNs exhibits three sharp bands at 1450, 1492 and 1604  $\text{cm}^{-1}$  assigned to C=C stretching vibration and two bands at 760 and 693  $\text{cm}^{-1}$  assigned to C-H bending vibration of the benzene ring of PS. The FTIR spectra confirm the encapsulation of silica by PS because any physically adsorbed PS macromolecules had been removed by Soxhlet extraction with toluene before FTIR measurement. A weak peak appearing at 800  $\text{cm}^{-1}$  is attributed to distortion vibration of aromatic C-H bond, which evidences the presence of DVB.

The difference in rheology between silica and SCCSN suspension's originates from the difference in extent of dispersion of the particles. A decrease of the linearity limit ( $\gamma_c$ ) with increasing particle concentration is associated with interaggregate links stronger than the aggregates themselves. The x and y exponents are extremely sensitive to particle dispersion, and a lower value of x suggests a better particle dispersion.<sup>40</sup> A positive x value of about 2.0 is usually revealed in filled polymer melts whose linear viscoelasticity is governed by the particle – particle

interaction.<sup>40</sup> In the silica suspensions, increasing  $\phi_{PS}$  is favorable for interconnection of silica aggregates via bridging of PS macromolecules, which somewhat stabilizes silica aggregates in the suspension.

## 4. Conclusions

Silica Nanoparticle of 32 – 98 nm in diameter has been prepared through miniemulsion polymerization. The dynamic rheology of SCCSNs suspended in PS solution is quite different from that of the naked silica suspension. Naked silica aggregates adsorb PS chains from the suspension, which, together with hydrogen bonding on the filler surface, leads to particle agglomeration responsible for the liquid-to-solid transition. SCCSNs are well dispersed in PS solution because hydrogen bonding between silica cores is completely eliminated. The SCCSN suspension forms a gel-like network. Structure at  $\phi_{SCCSN}=4.2$  vol%, which is ascribed to physically adsorbed PS macromolecules bridging individual SCCSN particles.

The addition of silica nanospheres to PEG hydrogels improved mechanical strength and decreased hydration kinetics. The compression of hydrogels suggests elastic and viscoelastic behaviors and the ability to recover back after deformation. Cell adhesion on hydrogel surface shows that silica provides sites for cell adhesion, and allows spreading, and proliferation. These properties can be tuned to obtain hydrogels with controlled cell adhesion to be used for various biomedical and biotechnological applications.

## References

1. Kang Y, Taton TA. Core/shell gold nanoparticles by self - assembly and crosslinking of micellar, block - copolymer shells. *Angewandte Chemie*. 2005, 117:413-416
2. Blomberg S, Ostberg S, Harth E, Bosman AW, Van Horn B, Hawker CJ. Production of crosslinked, hollow nanoparticles by surface - initiated living free - radical polymerization. *Journal of Polymer Science Part A: Polymer Chemistry*. 2002, 40:1309-1320
3. Caruso F, Caruso RA, Muhwald H. Production of hollow microspheres from nanostructured composite particles. *Chemistry of materials*. 1999, 11:3309-3314
4. Zhang K, Chen H, Chen X, Chen Z, Cui Z, Yang B. Monodisperse silica - polymer core - shell microspheres via surface grafting and emulsion polymerization. *Macromolecular materials and engineering*. 2003, 288:380-385
5. Tissot I, Reymond J, Lefebvre F, Bourgeat-Lami E. Sioh-functionalized polystyrene latexes. A step toward the synthesis of hollow silica nanoparticles. *Chemistry of materials*. 2002, 14:1325-1331
6. Gao D, Zhang Z, Wu M, Xie C, Guan G, Wang D. A surface functional monomer-directing strategy for highly dense imprinting of tnt at surface of silica nanoparticles. *Journal of the American Chemical Society*. 2007, 129:7859-7866
7. Fleming MS, Mandal TK, Walt DR. Nanosphere-microsphere assembly: Methods for core-shell materials preparation. *Chemistry of materials*. 2001, 13:2210-2216
8. Bartholome C, Beyou E, Bourgeat-Lami E, Chaumont P, Zydowicz N. Nitroxide-mediated polymerizations from silica nanoparticle surfaces:“Graft from” polymerization of styrene using a triethoxysilyl-terminated alkoxyamine initiator. *Macromolecules*. 2003, 36:7946-7952
9. Xu H, Cui L, Tong N, Gu H. Development of high magnetization fe<sub>3</sub>o<sub>4</sub>/polystyrene/silica nanospheres via combined miniemulsion/emulsion polymerization. *Journal of the American Chemical Society*. 2006, 128:15582-15583
10. Radhakrishnan B, Ranjan R, Brittain WJ. Surface initiated polymerizations from silica nanoparticles. *Soft Matter*. 2006, 2:386-396
11. Yu M, Lin J, Fang J. Silica spheres coated with yvo<sub>4</sub>: Eu<sup>3+</sup> layers via sol-gel process: A simple method to obtain spherical core-shell phosphors. *Chemistry of Materials*. 2005, 17:1783-1791



12. Kotal A, Mandal TK, Walt DR. Synthesis of gold–poly (methyl methacrylate) core–shell nanoparticles by surface - confined atom transfer radical polymerization at elevated temperature. *Journal of Polymer Science Part A: Polymer Chemistry*. 2005, 43:3631-3642
13. Savin DA, Pyun J, Patterson GD, Kowalewski T, Matyjaszewski K. Synthesis and characterization of silica - graft - polystyrene hybrid nanoparticles: Effect of constraint on the glass - transition temperature of spherical polymer brushes. *Journal of Polymer Science Part B: Polymer Physics*. 2002, 40:2667-2676
14. Lu C-H, Zhou W-H, Han B, Yang H-H, Chen X, Wang X-R. Surface-imprinted core-shell nanoparticles for sorbent assays. *Analytical chemistry*. 2007, 79:5457-5461
15. Caruso F, Muhwald H. Preparation and characterization of ordered nanoparticle and polymer composite multilayers on colloids. *Langmuir*. 1999, 15:8276-8281
16. Tsyalkovsky V, Klep V, Ramaratnam K, Lupitskyy R, Minko S, Luzinov I. Fluorescent reactive core–shell composite nanoparticles with a high surface concentration of epoxy functionalities. *Chemistry of Materials*. 2007, 20:317-325
17. Yin X, Tan Y, Gao Y, Song Y, Zheng Q. Viscoelasticity of shell-crosslinked core–shell nanoparticles filled polystyrene melt. *Polymer*. 2012, 53:3968-3974